Available online at www.sciencedirect.com
SCIENCE DIRECT
Polymer 46 (2005) 11829–11836
polymer
www.elsevier.com/locate/polymer

Compatibilization-like effect of reactive organoclay on the poly(L-lactide)/poly(butylene succinate) blends

Guang-Xin Chen, Hun-Sik Kim, Eung-Soo Kim, Jin-San Yoon *

Department of Polymer Science and Engineering, Inha University, Incheon 402-751, South Korea

Received 8 June 2005; received in revised form 6 October 2005; accepted 10 October 2005
Available online 26 October 2005

Abstract

The morphology of an incompatible polymer blend composed of poly(L-lactide) (PLLA) and poly(butylene succinate) (PBS) was examined by scanning and transmission electron microscopy, X-ray scattering, and X-ray photoelectron spectroscopy before and after the incorporation of an organoclay containing reactive functional groups, namely twice functionalized organoclay (TFC). TFC was prepared by treating Cloisite® 25A with (glycidoxypropyl)trimethoxy silane. When a small amount of TFC was incorporated into the PLLA/PBS blend, the clay layers became fully exfoliated and were located mainly in the PLLA phase. At the low clay content, the dispersed phase had an almost constant domain size comparing with the PLLA/PBS blend, which decreased sharply as the clay content was further increased. When the clay content became high, the clay layers were dispersed not only in the PLLA phase but also in the PBS phase with intercalated/exfoliated coexisting morphology. The reactive TFC was found to play an important role in the blend similar to the in situ reactive compatibilizer. The specific interaction between the TFC and the polymer matrix was quantified by the Flory–Huggins interaction parameter, B, which was determined by combining the melting point depression and the binary interaction model. The morphology of the PLLA/PBS/clay composites was analyzed by considering the interaction parameter.

Keywords: Blend; Epoxy groups; Poly(L-lactide)

1. Introduction

Polymer blending is an effective way of achieving a desirable combination of properties, which are often absent in single component polymers. However, a polymer blend often produces a material with poor mechanical properties as most polymer pairs are thermodynamically immiscible with each other [1]. Many studies have focused on enhancing the compatibility between the component polymers [2], either by adding a third component, which is miscible with both parent polymers [3], or by inducing a chemical reaction, leading to the modification of the polymer interface. The compatibilizers in situ formed are believed to be located preferentially at the interface [4–8].

Recently, clays have been used to improve thermal and mechanical [9–12], ablative [13], electrorheologically sensitive [14,15], stable electro-optical [16], corrosion protective [17], or conducting [18] properties of nanocomposites.

Some reports have shown that organoclays can act as compatibilizers for immiscible polymer blends [19–24]. Voulgaris and Petridis [20] reported that an organoclay contributed to the emulsification of a polystyrene/poly(ethyl methacrylate) blend. The domain size of the polystyrene/poly(methyl methacrylate) blend was reduced dramatically as a result of the incorporation of the organoclay [21]. The compatibilization by the excessive surfactant used to modify the clay and the increased viscosity were thought to be responsible for the reduced domain size. The two immiscible polymer chains co-existing between the intercalated clay platelets in polystyrene/polypropylene blend/clay composite were reported to behave like block copolymers that increase the compatibility between the two polymers [22]. Mehrabzadeh and Kamal [23] observed that the addition of 5 wt% clay to a high-density polyethylene/nylon6 blend reduced the dispersed nylon6 domain size. Recently, Khatua et al. [24] reported that the dispersed domain size in an incompatible nylon6/ethylene-propylene rubber blend was reduced by the presence of the organoclay. They showed that almost all the exfoliated clay platelets were localized in the nylon6 phase. The lower critical solution transition of the polystyrene/poly(vinyl methyl ether) blend was not altered significantly even when the organoclay content was as high as 4% [25,26].

* Corresponding author.
E-mail addresses: gxchen@eyou.com (G.-X. Chen), jsyoon@inha.ac.kr (J.-S. Yoon).

0032-3861/$ - see front matter © 2005 Elsevier Ltd. All rights reserved.
doi:10.1016/j.polymer.2005.10.056

However, the kinetics as well as the morphological development of phase separation of the blend are strongly influenced by the addition of the organoclay.

According to previous studies, the organoclay can enhance the compatibility between the component polymers in a polymer blend/clay composite in a similar manner to graft or block copolymers added deliberately as compatibilizers. The resulting fine morphology of the blend is expected to enhance the mechanical properties. Unfortunately, the mechanical properties have not been reported.

Therefore, the strength of the interaction between the polymer matrix and the clay particles need to be evaluated in order to predict the material properties and to obtain the optimal performance. This is because the mechanical properties of a polymer-based nanocomposite strongly depend on the homogeneity of the dispersion as well as the miscibility of the clay particles in the polymer matrix. Vaia and Giannelis [27,28] estimated the degree of the interaction between polymers and organically modified clays using the lattice model, and provided a guideline for an experimental investigation. Balazs et al. [29,30] also investigated the phase behavior of a binary polymer/clay mixture based on their theoretical framework and predicted a phase diagram to accommodate the various characteristics of the polymer and the clay surface.

The twice-functionalized organoclay (TFC), which is an organoclay containing epoxy groups, was synthesized in this laboratory and found to have a high degree of exfoliation in a PLLA matrix as a result of a chemical reaction between the epoxy groups and the polymer [31–33].

The main aim of this study was to examine the dispersion and the role of the organoclay in the immiscible polymer blend composed of poly(L-lactide) (PLLA) and poly(butylenes succinate) (PBS). Because the TFC could react with both PLLA and PBS, the in situ formed polymer-clay hybrid could play a role as a compatibilizer between the PLLA and PBS. The interaction between the clay and the polymers in the PLLA/PBS/TFC composite was described using the thermodynamic interaction energy density, B, based on the classical Flory–Huggins theory [34]. Differential scanning calorimetry (DSC) was used to determine the B values of the binary PLLA/TFC and PBS/TFC composites by combining the melting point depression with the binary interaction model, which was originally used to evaluate the specific interaction between two different chemical species.

2. Experimental

2.1. Materials

The poly(L-lactide) (PLLA) was purchased from Cargill Dow Co. with a molecular weight of 2.4×10^5 g/mol. The poly(butylene succinate) (PBS) was obtained from Irae Chemical Co., Korea, with a molecular weight of 5×10^4 g/mol, as reported by the manufacturer. The organoclay, Cloisite® 25A (C25A), was purchased from Southern Clay Product Inc. The twice functionalized organoclay (TFC) with the epoxy groups was prepared by treating the C25A with (glycidoxypropyl)trimethoxy silane. The grafted amount of the epoxy group was 0.36 mmol/g [31].

2.2. Composites preparation

The PLLA/PBS/clay composites were prepared by melt compounding the polymers with the clays at 180 °C for 10 min using a Brabender internal mixer. Weight ratio of the PLLA/PBS was kept constant at 75/25. The dried pellets were hot pressed at 180 °C for 1 min at 4 atm to prepare sheets with a thickness of approximately 0.5 mm.

2.3. Measurements

The morphology of the blends was observed using scanning electron microscopy (SEM, JXA-840) at an accelerating voltage of 25 kV. The blend samples were fractured at liquid nitrogen temperature. The cross sectional area (A_i) of each particle in the SEM micrograph was measured and then converted into the diameter (D_i) of a circlet with the same cross sectional area using the following equation: $D_i=2(A_i/\pi)^{1/2}$. The number-average diameter (D) was then obtained by $D=\Sigma D_i/N$ where N is the total number of the dispersed domains observed in the SEM images.

Transmission electron microscopy (TEM, 2000 EX-II instrument, JEOL, Tokyo, Japan), which was operated at an accelerating voltage of 100 kV, was used to observe the nanoscale structures of the various composites. All the ultrathin sections (less than 100 nm) were microtomed using a Super NOVA 655001 instrument (Leica, Swiss) with a diamond knife.

X-ray diffraction (XRD, Philips PW1847 X-ray diffractometer) was carried out with a reflection geometry and Cu K_α radiation (wavelength $\lambda=0.154$ nm) operated at 40 kV and 100 mA. The data were collected within the range of scattering angles (2θ) of 2–10°.

X-ray photoelectron spectroscopy (XPS) was carried out on a VG Scientific ESCALAB 200A (UK) spectrometer using magnesium K_α (1253.6 eV) X-rays as the radiation source. The survey spectra were collected over a range of 0–1150 eV using an analyzer pass energy of 50 eV.

Differential scanning calorimetry (DSC) was carried out using a Perkin–Elmer 7 instrument. Dry nitrogen gas was allowed to flow through the DSC cell at a rate of 20 ml/min. The DSC was calibrated using indium as the standard. The equilibrium melting temperature (T_m^0) was measured by heating the sample to 190 °C, and maintaining it at that temperature for 15 min in order to ensure complete melting of the polymer crystals. The sample was then quenched to the crystallization temperature T_c, held at that temperature for at least 5 h to ensure complete crystallization, and then heated at a heating rate of 20 °C/min.

Tensile specimens with dimension of 10 mm (width)×50 mm (length)×1 mm (thickness) were prepared from the hot pressed sheets. The specimens were subjected to uniaxial elongation at room temperature. All the experiments were

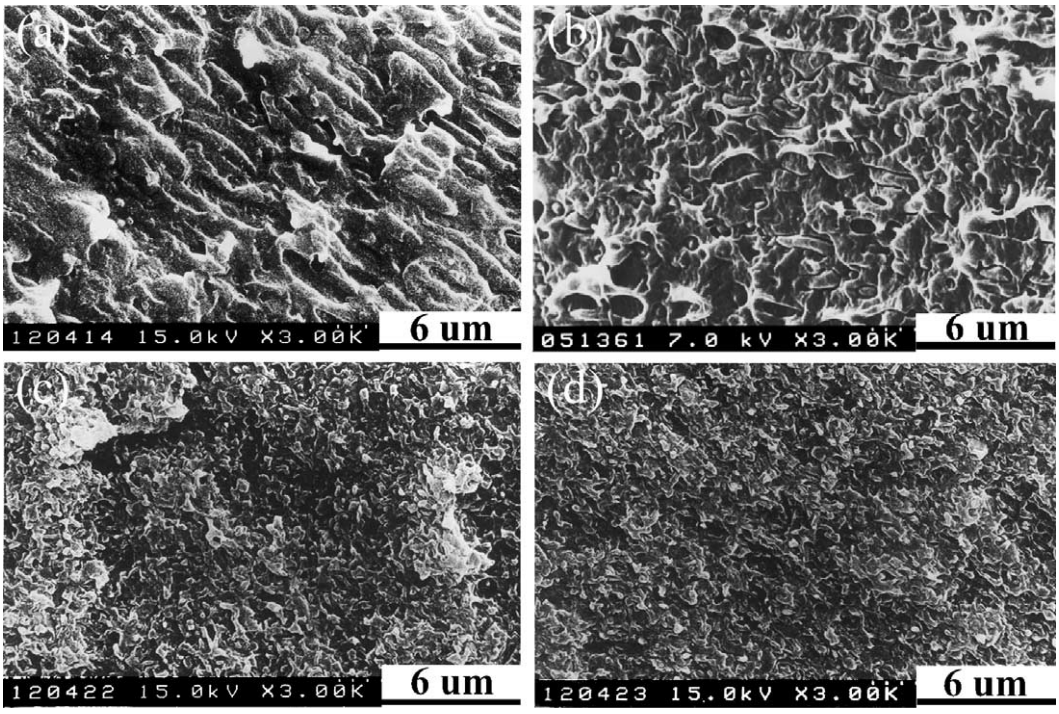

Fig. 1. SEM micrographs of the PLLA/PBS blends with various amounts of TFC (a) 0, (b) 0.5, (c) 2, (d) 5 wt%.

carried out with a UTM, Hounsfield test equipment with a cross head speed of 20 mm/min.

3. Results and discussion

3.1. Morphology

Fig. 1 shows SEM images of the PLLA/PBS blends containing various amounts of the twice-functionalized organoclay (TFC). The domain size of the dispersed PBS phase decreased with increasing TFC content. The dependence of the domain size on the TFC content is shown in Fig. 2. When the TFC content was <0.5 wt%, the domain size of the dispersed PBS phase decreased slightly with increasing TFC content (stage I). However, the domain size became much smaller when the TFC content was 2 wt% (stage II). Finally a slow but gradual decrease in the domain size was observed with further increases in the TFC content (stage III).

Khatua et al. [24] also reported that the domain size of the dispersed phase of a poly(ethylene-*co*-propylene) rubber (EPR)/nylon 6 blend decreased with increasing clay content. However, the decrease in the domain size was significant even when 0.5 wt% of the clay was incorporated, which is in contrast to the results of this study. Khatua et al. [24] attributed this decrease in domain size to exfoliated clay platelets in the polymer blend effectively preventing the coalescence of the dispersed domains. According to their TEM images, the organoclay platelets were not located near the interface between the EPR phase and the nylon 6 one. Therefore, the decrease in the domain size of the dispersed phase was not caused by a compatibilizing effect of the clay.

The initial sharp decrease followed by the slow and gradual decrease of the domain size with increasing clay content can also be seen in the typical emulsification curve of immiscible polymer blends with a block or graft copolymer as a compatibilizer. Therefore, the stage I observed in this study is not observed in normal incompatible polymer blends as well as in the EPR/nylon 6/clay composite.

In order to closely examine this peculiar gradual decrease in domain size, the intercalation capabilities of the individual polymer and the polymer blend with clay were compared by XRD, as shown in Figs. 3 and 4. Fig. 3 shows the XRD patterns of Cloisite® 25A, TFC, PLLA/TFC, and PBS/TFC composites. The TFC content in the composites was 5 wt%. The TFC exhibited its 2θ peak at 4.72°, which corresponds to a d_{001}

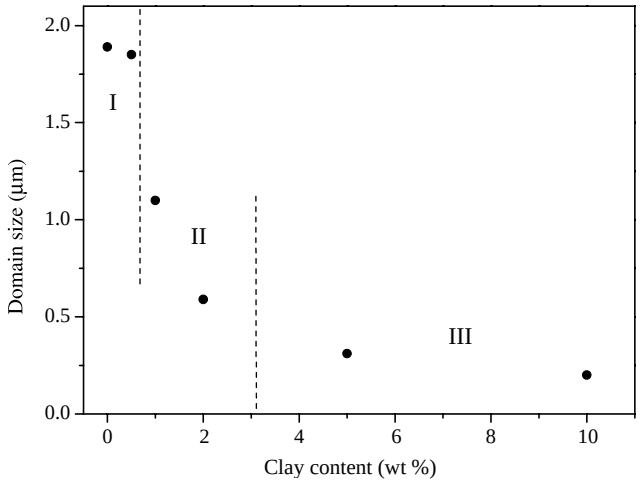

Fig. 2. Average PBS domain size as a function of the TFC content.

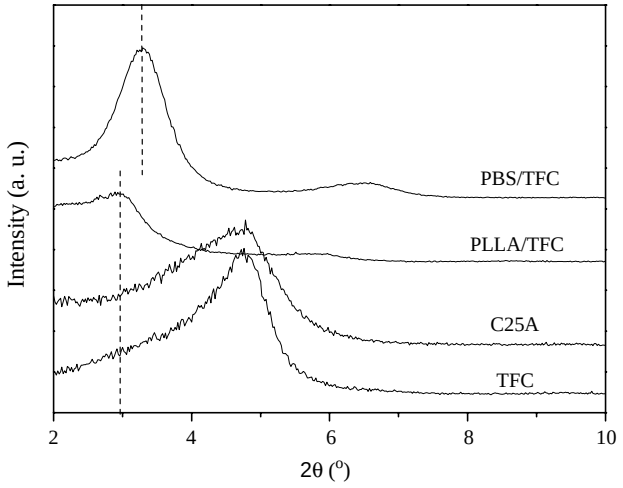

Fig. 3. XRD patterns of the Cloisite 25A, TFC, PLLA and PBS composites with 5 wt% TFC.

spacing of 1.86 nm. The insertion of PLLA or PBS chains between the clay layers were confirmed by the increase in the d_{001} basal spacing from 1.86 to 3.04 and 2.68 nm for the PLLA/TFC and PBS/TFC composites, respectively. This observation suggests that the degree of intercalation of the PLLA/TFC composite is higher than that of the PBS/TFC composite [35].

The PLLA/PBS weight ratio was fixed to 75/25 and the TFC content in the blend was varied from 0 to 10 wt%. Fig. 4 shows the XRD patterns of the resulting PLLA/PBS/TFC composites. The XRD scattering peak was not observed until the TFC content became higher than 2%. The d_{001} spacing of the PLLA/PBS/TFC composites was unaffected by the TFC content, and was 2.98, 2.96, and 2.96 nm for TFC contents of 2, 5 and 10 wt%, respectively. The d_{001} spacing of the PLLA/PBS/TFC composites was somewhere in between those of the PLLA/TFC and PBS/TFC composites. This shows that both PLLA and PBS molecules were inserted between the TFC layers in the PLLA/PBS/TFC composites. TEM imaging of the composites was carried out on the PLLA/PBS blend with different TFC levels in order to register a detailed icon for the location of the clay layers in the polymer blend (Fig. 5). It was difficult to distinguish the PLLA phase from the PBS domain because there was little contrast difference between them. However, two points are worth noting in Fig. 5. First, the clay platelets are well dispersed throughout the PLLA/PBS/TFC composite without any of the aggregation or tactoid formation that is indicative of a fully exfoliated morphology of the composite. Second, the exfoliated clay layers are not uniformly distributed in the composite as in other exfoliated polymer clay nanocomposites [36]. The TFC layers are very scarce in the domain encircled by the dotted line in Fig. 5(a), which corresponds to the TEM image of the composite containing 0.5 wt% TFC. According to previous studies [31–33,37], TFC is more easily exfoliated in a PLLA matrix than in a PBS matrix. Therefore, it is reasonable to assume that the TFC layers located mainly in the PLLA phase when a small amount of TFC is incorporated into the PLLA/PBS/TFC composite. A discernible TFC layer begins to be dispersed in the PBS phase when the TFC content exceeds a certain threshold. Therefore, it is believed that the domain containing a few TFC layers encircled by the dotted line corresponds to the PBS phases. The domain size is in agreement with the average diameter shown in the corresponding SEM micrographs. Most of the TFC layers are in the PLLA phase with full exfoliation, as shown in Fig. 5(b). However, when the TFC content was increased to 5 wt%, the TFC layers were well dispersed not only in the PLLA phase but also in the PBS phase with intercalated/exfoliated coexisting morphology, as shown in Fig. 5(c). The location of the TFC layers is shown by the XPS analyses in Fig. 6.

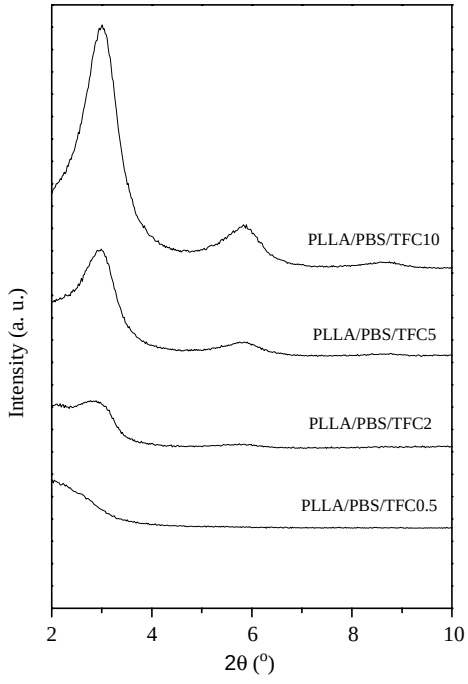

Fig. 4. XRD patterns of the PLLA/PBS nanocomposites with 0.5, 2, 5 and 10 wt% of the TFC.

The XPS spectra of the PLLA/PBS/TFC composite show the presence of three elements, C, O, and Si. C and O were attributed to the matrix polymer and the surfactant used for the production of the Cloisite® 25A, while Si was associated with the TFC layers. Fig. 6 shows the XPS spectra of the PLLA/PBS/TFC composite with 0.5 wt% TFC after two days of Soxhlet extraction of the PLLA phase using boiling tetrahydrofuran (THF). It should be noted that the peaks for C and O were detected, while no Si peak was observed in the XPS spectrum of the residual fraction, which is the phase rich in PBS, after the Soxhlet extraction. In contrast, the Si peak was observed in the XPS spectrum of the fraction that had been removed from the PLLA/PBS/TFC composite by Soxhlet extraction. This fraction should be rich in PLLA. However, when the TFC content of the PLLA/PBS/TFC composite was 5 wt%, the XPS peak for Si was detected not only in the fraction removed by the Soxhlet extraction but also in the residual fraction, as demonstrated in Fig. 6. These results show that when the TFC content was very low, the TFC layers were located almost exclusively in the PLLA phase. As the TFC

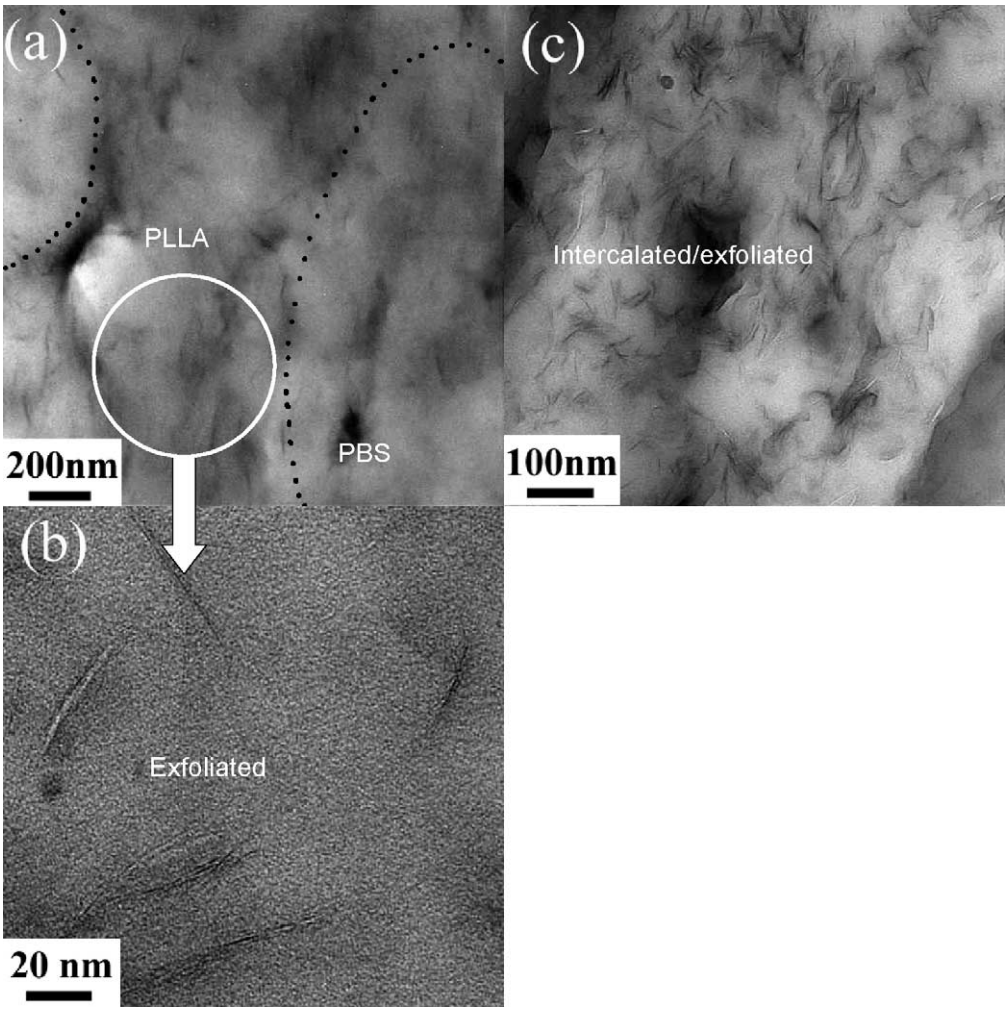

Fig. 5. TEM micrographs of the PLLA/PBS blends with TFC (a) 0.5 wt%, lower magnification, (b) 0.5 wt%, higher magnification, (d) 5 wt%.

content exceeded the level required to complete fill up the PLLA phase, a surplus amount of the TFC layers began to be dispersed in the PBS phase.

The higher partition of the clay layers into the PLLA matrix was attributed to the more favorable compatibility between the TFC and PLLA than between the TFC and PBS. The higher degree of exfoliation in the PLLA/TFC composite compared with that in PBS/TFC composite highlights the more favorable compatibility in the former composite.

Because the clay layers were located exclusively in the PLLA phase at low TFC content and few of the clay layers were located in the interface between the PLLA phase and the PBS phase, the clay layers did not hinder the coalescence of the dispersed PBS domains. This is why the incorporation of a small amount of TFC did not significantly reduce the domain size of the PBS phase, while the domain size of the dispersed phase in many other polymer blend/clay composites decreased drastically even when the clay content was as low as 0.5 wt%.

The dispersed domain size decreased sharply as the TFC content was increased. According to the TEM image shown in Fig. 5(c), the clay layers were well dispersed in the polymer blend. Therefore, some of them should be located at

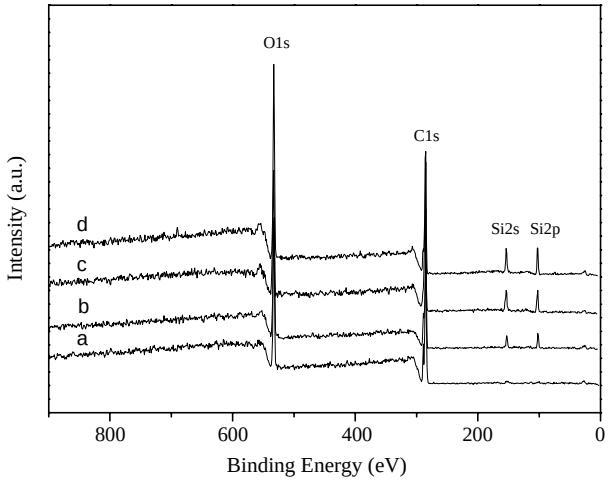

Fig. 6. XPS spectra of the PLLA/PBS/TFC composites with TFC (a) 0.5 wt%, residual PBS after 24 h of etching in THF, (b) 0.5 wt%, removed PLLA after 24 h of etching in THF, (c) 5 wt%, after 24 h of etching in THF, (d) 5 wt%, after 24 h of etching in THF.

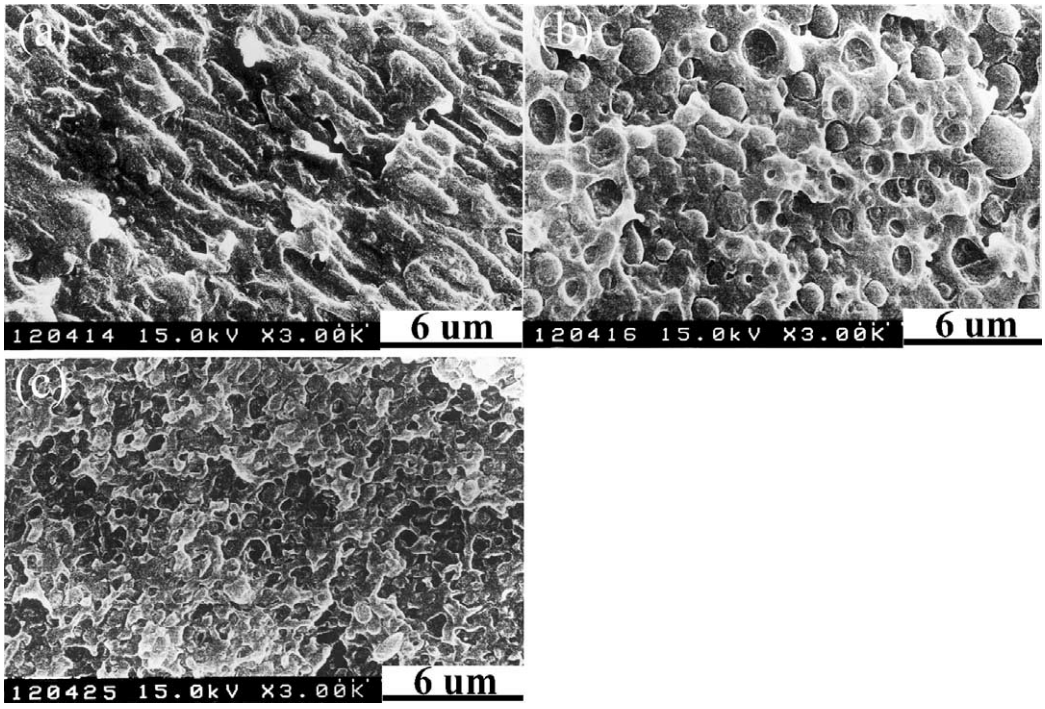

Fig. 7. SEM micrographs of the PLLA/PBS blends with various amounts of Cloisite 25A (a) 0, (b) 5, (c) 10 wt%.

the interface in order to prevent coalescence of the dispersed domains and contribute to the reduction in the domain size. The PLLA-silicate-PBS hybrid formed in situ during melt compounding should also played an important role in reducing the dispersed domain size, in a similar manner to that in in situ reactive compatibilization in incompatible polymer blends. PLLA/PBS/C25A composites were prepared to examine the effects of the functional groups on the domain size and mechanical properties of the polymer blend. Fig. 7 shows SEM micrographs of the PLLA/PBS blends with 0–10 wt% of C25A. The dispersed domain size was 1.6 μm, which was similar to that in the absence of C25A (1.8 μm), even though the C25A content was as high as 5 wt%. The PBS domain size in the PLA/PBS/C25A composites decreased when the C25A content was increased to 10 wt%, which was possibly due to the increased viscosity as a result of clay incorporation [22–24]. This is in sharp contrast to the PLLA/PBS/TFC system, where the dispersed domain size was 0.59 μm in the presence of 2 wt% TFC. Therefore, the functional groups of TFC played an important role in reducing the dispersed domain size and acted similar as a compatibilizer in the PLLA/PBS blend. Accordingly, the interaction parameters of the corresponding composites were determined in order to clarify the reason why the TFC was more compatible with PLLA than with PBS.

3.2. Interaction parameter

An evaluation of the specific interaction between the polymer matrix and the silicate layers can be made by combining the melting point depression with the binary interaction model for the heat of mixing [38]. The melting peak temperature and heat of fusion of the PLLA/TFC composites decreased with increasing TFC content, indicating that a specific interaction exists between the PLLA and TFC. The relationship between the melting point depression and the interaction energy parameter in the mixture can be described by the following equation [39]:

$$T_m^0 - T_{mix}^0 = -\frac{BV_{iu}}{\Delta H_{iu}} T_m^0 (1-\phi_i)^2 \quad (1)$$

where T_m^0 and T_{mix}^0 are the equilibrium melting points of PLLA and the mixture, respectively. $\Delta H_{iu}/V_{iu}$ is the heat of fusion of PLLA per unit volume, Φ_i is the volume fraction of PLLA, and B is the interaction energy density between the two components. The overall interaction energy density, B, can be obtained from the slope of the plot of $T_m^0 - T_{mix}^0$ as a function of $(1-\Phi_i)^2$.

The equilibrium melting temperatures of pure PLLA and PLLA/TFC composites were obtained by using the Hoffman-Weeks plots, as shown in Fig. 8, and the results are shown in Table 1. Fig. 9 gives the melting point depression of PLLA in the PLLA/TFC composites as a function of the PLLA content. The value of B in Eq. (1) was determined from the slope of the straight line shown in Fig. 9. B was estimated to be -41.1 cal/cm^3 by assigning V_{iu} and ΔH_{iu} values of 1.89×10^5 cm^3/mol and 41.2×10^5 cal/mol, respectively, indicating that the TFC interacted favorably with the PLLA.

The heat of mixing, ΔH_{mix}, of a multi-component system can be described in terms of the binary interaction parameters as follows:

$$\Delta H_{mix} = V \sum_i \sum_j B_{ij} \phi_i \phi_j \quad (2)$$

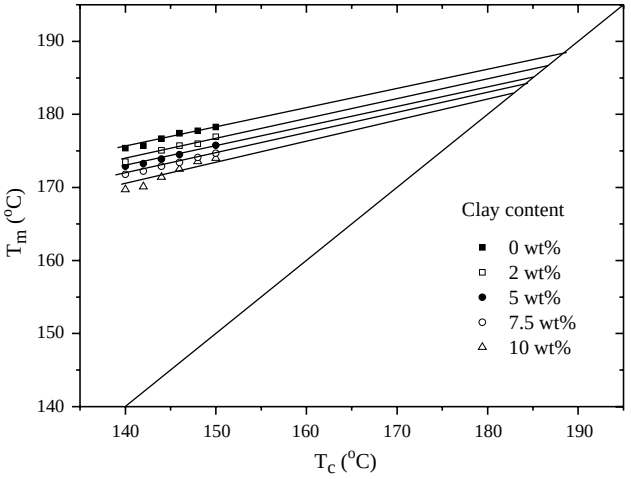

Fig. 8. Hoffman–Weeks plot for the PLLA/TFC composite with various clay contents.

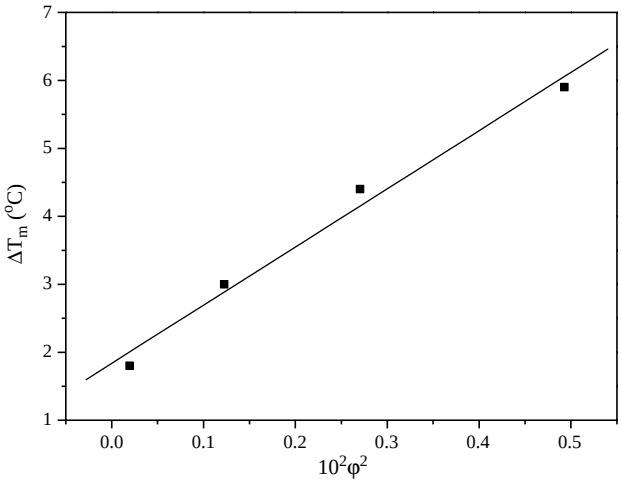

Fig. 9. Plot of the equilibrium melting point of PLLA in the PLLA/TFC composite.

where V is the volume, B_{ij} is the interaction energy density, and Φ_i and Φ_j are the volume fraction of components i and j in the mixture, respectively. In case of binary mixtures, $\Delta H_{mix}=0$ becomes the criterion for predicting the boundary between single-phase and multiphase behavior.

The same method was used to determine the interaction energy density between PBS and TFC, which was calculated to be -1.5 cal/cm^3. The estimated interaction parameters of the pairs suggested that the interaction between the PLLA and TFC was much more favorable than that between PBS and TFC.

3.3. Mechanical properties

Table 2 summarizes the tensile properties of the PLLA/PBS/TFC. The tensile properties of the PLLA/PBS/C25A composites are also shown for comparison. According to Table 2, the addition of C25A to the PLLA/PBS blend significantly increased the tensile modulus. This demonstrated that C25A acted as a reinforcing filler on account of its high aspect ratio and platelet structure. However, the elongation at break of the PLLA/PBS blend decreased precipitously as a result of C25A incorporation. The tensile modulus of the PLLA/PBS/TFC composites also increased with increasing clay content, and this increase was more pronounced compared with that of the PLLA/PBS/C25A composites. This is believed to be due to the epoxy functional groups of TFC, which promoted an interaction between the clay and the polymer matrix through a chemical reaction [31].

In many cases [40], an increase in the tensile modulus of various polymers by compounding them with clay reduces the elongation at break. However, Table 2 shows that both the tensile modulus and the elongation at break of the PLLA/PBS blend increased when the TFC content in the composite was increased to 10 wt%. The specimens containing TFC showed increased necking in addition to the formation of a prominent fibrillar fracture surface, whereas those with C25A exhibited brittle fracture without necking. This shows that the chemical bonds between the TFC and the two component polymers strengthened the interfacal interaction. Therefore, TFC acted as a compatibilizer in the PLLA/PBS/TFC composites.

Table 1
Table1 Measured equilibrium melting temperatures of the PLLA/TFC blends

PLLA/TFC (wt/wt)	T_m^0 (°C)
100/0	188.2
98/2	186.4
95/5	185.2
92.5/7.5	183.8
90/10	182.3

4. Conclusions

Epoxy groups were introduced to Cloisite® 25A by treating the clay with (glycidoxypropyl)trimethoxy silane to produce the twice functionalized organoclay(TFC). When a small amount of TFC was incorporated in a PLLA/PBS blend, the clay layers were fully exfoliated and were located almost exclusively in the PLLA phase. The domain size of the dispersed PBS phase did not change considerably when

Table 2
Tensile properties of the PLLA(75)/PBS(25)/clay nanocomposites

Samples	Modulus (MPa)	Elongation at break (%)	Yield strength (MPa)
PLLA	2214.7	6.9	64.6
PBS	326.3	320.6	32.1
PLLA/PBS	1075.2	71.8	44.7
PLLA/PBS/C25A2	1364.6	4.4	42.8
PLLA/PBS/C25A5	1616.6	4.1	44.4
PLLA/PBS/C25A10	1940.1	3.6	45.5
PLLA/PBS/TFC2	1407.9	75.5	45.2
PLLA/PBS/TFC5	1624.6	100.6	45.8
PLLA/PBS/TFC10	1990.3	118.1	46.7

the TFC content was 0.5 wt%. However, as the TFC content increased, the clay layers were dispersed in both the PBS and PLLA phases, and the domain size of the dispersed PBS phase grew significantly smaller. The Flory–Huggins interaction parameters, B, were estimated to be -41.1 and -1.5 cal/cm^3 for the PLLA/TFC and PBS/TFC system, respectively, suggesting that TFC was highly compatible with PLLA. The addition of TFC to the PLLA/PBS blend not only improved the tensile modulus but also improved the elongation at break, while the incorporation of C25A to the same polymer blend increased the tensile modulus but at the cost of the elongation at break.

Acknowledgements

This work was supported by grant No. R01-2002-000-00146-0 from the interdisciplinary research program of the KOSEF. The support for G. X. C. from the Brain Korea 21 project in 2003 is gratefully acknowledged.

References

[1] Folkes MJ, Hope PS, editors. Polymer blends and alloys. New York: Blackie Academic and Professional; 1993.
[2] Paul DR, Bucknall CB, editors. Polymer blends. New York: Wiley; 2000.
[3] Utracki L. Polymer alloys and blends. New York: Hanser; 1989.
[4] Majumdar B, Keskkula H, Paul DR. Polymer 1994;35:1386.
[5] Majumdar B, Keskkula H, Paul DR. Polymer 1994;35:1399.
[6] Chen GX, Liu JJ. J Appl Polym Sci 2000;76:799.
[7] Chen GX, Dong WF, Liu JJ. J Mater Sci 2002;37:1215.
[8] Chen GX, Liu JJ. J Mater Sci 1999;34:4375.
[9] Maiti P, Yamada K, Okamoto M, Ueda K, Okamoto K. Chem Mater 2002; 14:4654.
[10] Chen GX, Yoon JS. Polym Degrad Stab 2005;88:206.
[11] Chen GX, Yoon JS. Polym Inter 2005;54:939.
[12] Chen GX, Hao GJ, Guo TY, Zhang BH. J Mater Sci Lett 2002;21:1587.
[13] Vaia RA, Price G, Ruth PN, Nguyen HT, Lichtenhan J. Appl Clay Sci 1999;15:67.
[14] Kim JW, Noh MH, Choi HJ, Lee DC, Jhon MS. Polymer 2000;41:1229.
[15] Park JH, Lim YT, Park OO. Macromol Rapid Commun 2001;22:616.
[16] Kawasumi M, Hasegawa N, Usuki A, Okada A. Appl Clay Sci 1999; 15:93.
[17] Yeh JM, Liou SJ, Lin CY, Cheng CY, Chang YW, Lee KR. Chem Mater 2002;14:154.
[18] Lee D, Lee SH, Char K, Kim J. Macromol Rapid Commun 2000;21:1136.
[19] Chen GX, Yoon JS. J Polym Sci, Part B: Polym Phys 2005;43:478.
[20] Voulgaris D, Petridis D. Polymer 2002;43:2213.
[21] Gelfer MY, Song HH, Liu L, Hsiao BS, Chu B, et al. J Polym Sci, Polym Phys 2003;41:44.
[22] Wang Y, Zhang Q, Fu Q. Macromol Rapid Commun 2003;24:231.
[23] Mehrabzadeh M, Kamal MR. Can J Chem Eng 2002;80:1083.
[24] Khatua BB, Kim HY, Kim JK. Macromolecules 2004;37:2454.
[25] Yurekli K, Karim A, Amis EJ, Krishnamoorti R. Macromolecules 2003; 36:7256.
[26] Yurekli K, Karim A, Amis EJ, Krishnamoorti R. Macromolecules 2004; 37:507.
[27] Vaia RA, Giannelis EP. Macromolecules 1997;30:7990.
[28] Vaia RA, Giannelis EP. Macromolecules 1997;30:8000.
[29] Balazs AC, Singh C, Zhulina E. Macromolecules 1998;31:8370.
[30] Lyatskaya Y, Balazs AC. Macromolecules 1998;31:6676.
[31] Chen GX, Choi JB, Yoon JS. Macromol Rapid Commun 2005;26:183.
[32] Chen GX, Kim HS, Shim JH, Yoon JS. Macromolecules 2005;38:3738.
[33] Chen GX, Yoon JS. Macromol Rapid Commun 2005;26:899.
[34] Riedl B, Prudhomme RE. Polym Eng Sci 1985;24:1291.
[35] Choi SB, Lee KM, Han CD. Macromolecules 2004;37:7649.
[36] Okada O, Kawasumi M, Usuki A, Kojima Y, Kurauchi T, Kamigaito O. Mater Res Soc Symp Proc 1990;171:45.
[37] Chen GX, Kim ES, Yoon JS. J Appl Polym Sci 2005;98:1727.
[38] Lim SK, Kim JW, Chin I, Kwon YK, Choi HJ. Chem Mater 2002;14: 1989.
[39] Nishi T, Wang TT. Macromolecules 1975;8:909.
[40] Pinnavaia TJ, Beall GW. Polymer–clay nanocomposites. New York: Wiley Series in Polymer Science; 2000.